

# Using the Outer Coordination Sphere to Tune the Strength of Metal Extractants

Ross S. Forgan,<sup>†</sup> Benjamin D. Roach,<sup>†</sup> Peter A. Wood,<sup>†</sup> Fraser J. White,<sup>†</sup> John Campbell,<sup>‡</sup> David K. Henderson,<sup>†</sup> Eduardo Kamenetzky,<sup>‡</sup> Fiona E. McAllister,<sup>†</sup> Simon Parsons,<sup>†</sup> Elna Pidcock,<sup>§</sup> Patricia Richardson,<sup>†</sup> Ronald M. Swart,<sup>‡</sup> and Peter A. Tasker<sup>\*,†</sup>

<sup>†</sup>School of Chemistry, University of Edinburgh, Edinburgh EH9 3JJ, U.K.

<sup>‡</sup>Cytec Industries, 1937 West Main Street, Stamford, Connecticut 06904-0060, United States

<sup>§</sup>Cambridge Crystallographic Data Centre (CCDC), 12 Union Road, Cambridge CB2 1EZ, U.K.

**S** Supporting Information

**ABSTRACT:** A series of 3-substituted salicylaldoximes has been used to demonstrate the importance of outer-sphere interactions on the efficacy of solvent extractants that are used to produce approximately one-quarter of the world's copper. The distribution coefficient for extraction of copper by 5-*tert*-butyl-3-*X*-salicylaldoximes ( $X = \text{H, Me, }^t\text{Bu, NO}_2, \text{Cl, Br, OMe}$ ) varies by more than two orders of magnitude. X-ray structure determinations of preorganized free ligand dimers (10 new structures are reported) indicate that substituents with a hydrogen-bond acceptor atom attached to the 3-carbon atom, *ortho* to the phenolic oxygen, buttress the intermolecular hydrogen bond from the oximic proton. Density functional theory calculations demonstrate that this hydrogen-bond buttressing is maintained in copper(II) complexes and contributes significantly to their relative stabilities in energy-minimized gas-phase structures. A remarkable correlation between the order of the calculated enthalpies of formation of the copper complexes in the gas phase and the observed strength of the ligands as copper solvent extractants is ascribed to the low solvation energies of species in the water-immiscible phase and/or the similarities of the solvation enthalpies of the preorganized ligand dimers and their copper(II) complexes.

## INTRODUCTION

Solvent extraction provides a very efficient way to achieve concentration and separation in extractive hydrometallurgy.<sup>1</sup> In the high-boiling nonpolar solvents preferred by industry, intermolecular forces between extractants, particularly hydrogen bonding, contribute very significantly to the stability of complexes formed in the water-immiscible phase. Extraction by organic derivatives of phosphorus(V) acids, e.g., by the commercial reagent bis(2-ethylhexyl)phosphoric acid (D2EHPAH), is often associated with the retention of strong interligand hydrogen bonding and the formation of eight-membered *pseudochelate* rings, as in Figure 1a.<sup>1,2</sup> Consequently, unusual anti-Irving–Williams<sup>3</sup> orders of stability of divalent first-row transition-metal complexes are observed,<sup>2</sup> and D2EHPAH shows selectivity for dications favoring tetrahedral geometry. A plant using D2EHPAH for the hydrometallurgical recovery of zinc on a 150 000 tonne per annum scale has been opened recently.<sup>4,5</sup>

In this paper, we consider in more detail how interactions in the *outer coordination spheres* of complexes can be used to control the strength and selectivity of metal extraction.<sup>6</sup> Such an approach extends the principles of supramolecular chemistry to processes that are already used on kilotonne scales in extractive hydrometallurgy. We focus on hydrogen bonding between salicylaldoxime extractants, which currently accounts<sup>7,8</sup> for between 20 and 30% of the world's production of copper. Their strength and selectivity for copper(II) arises from the stability of the 14-membered pseudomacrocyclic hydrogen-bonded assembly (Figure 1b), which provides a cavity of nearly ideal size for the

copper(II) ion.<sup>9</sup> This motif can also be observed in preorganized ligand dimers (Figure 2), which have planar “stepped” structures,<sup>9</sup> and we are particularly interested in defining to what extent “buttressing” of the interligand hydrogen bonding, by incorporating electronegative substituents in the 3 position (Figure 2), contributes to the stability of these ligand dimers and their copper(II) complexes.

A target for this work was to increase the strength of the extractants. While the strength of the current commercial reagents is almost ideal<sup>1</sup> for treating feed solutions containing up to 5 g L<sup>-1</sup> copper, obtained from heap leaching of oxidic ores, pH adjustment<sup>10</sup> may be needed to obtain good recovery from more concentrated feeds, and they are too weak to recover other divalent base metals.<sup>11</sup> Substitution on the benzene ring is known to affect the copper-binding properties of phenolic oximes; 3-nitro-2-hydroxy-5-nonylbenzophenone oxime ( $R = \text{C}_9\text{H}_{19}$ ,  $R' = \text{C}_6\text{H}_5$ ,  $X = \text{NO}_2$  in Figure 1b) extracts<sup>12</sup> copper at lower pH than its non-NO<sub>2</sub>-substituted analogue, and compounds with 3-chloro substituents ( $X = \text{Cl}$  in Figure 1b) were found<sup>13</sup> by General Mills Ltd. to have high extractant strength, providing a reagent for copper recovery from highly acidic chloride streams. Until recently, an empirical approach has been used to study the effects of substitution, leading to the view that groups that increase the acidity of phenol groups enhance the extractant strength.<sup>14</sup> This conclusion pays no attention to (i) the effects of

Received: January 24, 2011

Published: April 21, 2011

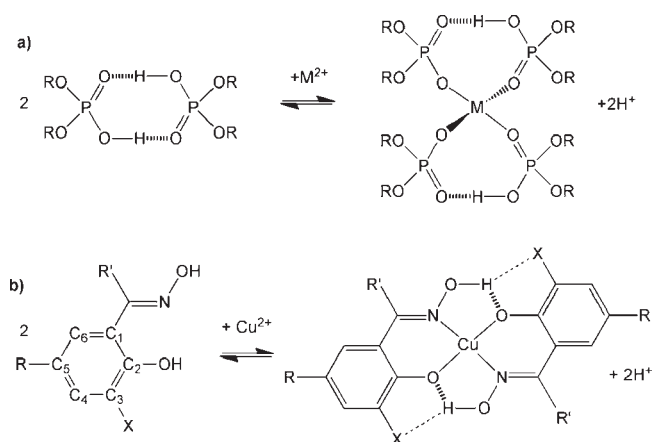


**Figure 1.** Examples of “pH-swing” extractants<sup>2</sup> (LH). Formation of (a) 8-membered pseudochelate rings by diesters of phosphoric acid such as D2EHPAH (R = 2-ethylhexyl), which function by the equilibrium  $2nLH_{org} + M^{n+} \rightleftharpoons [ML_n(LH)_n]_{org} + nH^+$ , and (b) 14-membered pseudomacrocycles by the 5-alkyl-substituted salicylaldoxime derivatives used in copper recovery, equilibrium  $2LH_{org} + M^{2+} \rightleftharpoons [ML_2]_{org} + 2H^+$ .

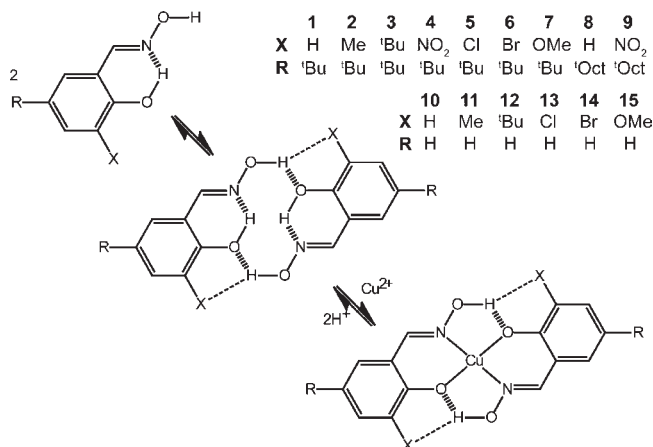
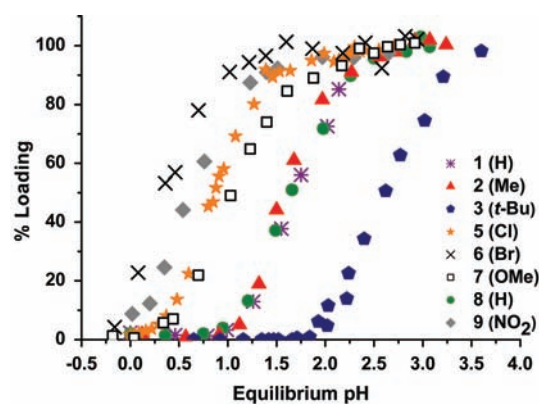


**Figure 2.** Possible buttressing of the interligand hydrogen bonding by 3-substituents, X, in the formation of dimers and pseudomacrocyclic copper(II) complexes of the salicylaldoximes, 1–15, used in this study.

substituents on the electronic properties of the donor atoms, which form bonds to the copper atom, and (ii) the influence that groups in the 3 position might have on the strength of the interligand hydrogen bonding (Figure 2), which contributes to the stability of the resulting pseudomacrocyclic complexes.<sup>15,16</sup>

In a recent communication,<sup>17</sup> we demonstrated that 3-substitution incorporating hydrogen-bond acceptors (X = Cl, OMe, etc., in Figure 2) appears to “buttress” the interligand hydrogen bonding in salicylaldoxime complexes, leading to increases in their strength as copper(II) extractants. The work presented in this paper extends the range of substituents and uses a combination of techniques to consider the relative importance of their effects on hydrogen-bond buttressing and other properties, for example, ligand acidity, which impact their strength as metal extractants.<sup>14</sup> An understanding of the supramolecular and outer-sphere coordination chemistry of extractants in nonpolar solvents is a prerequisite for the rational tuning of the reagent strength and selectivity to meet the requirements of a particular flowsheet.



L	1	2	3	5	6	7	8	9
$pH_{0.5}$	1.68	1.67	2.64	0.91	0.42	1.09	1.73	0.70

**Figure 3.** pH profiles and  $pH_{0.5}$  values for copper loading by 0.01 M chloroform solutions of L1–L9 from equal volumes of 0.01 M aqueous solutions of copper sulfate (100% copper loading based on the formation of a 1Cu:2L complex).

## RESULTS AND DISCUSSION

**Solvent Extraction.** Ligands 1–9 and 14 were successfully synthesized<sup>18–21</sup> in good yields (see the Supporting Information, S2) on the gram scale (10 is available commercially, and the syntheses of 11–13 and 15 have been reported by us previously).<sup>22</sup> Copper-loading experiments<sup>11</sup> were carried out to assess the relative “strengths” of 1–9 as solvent extractants. The low solubility of 4 prevented us from recording copper(II) loading data under the conditions (see Figure 3), which were used for the other ligands. In order to define the influence of 3-nitro substitution on the reagent strength, we used 9, a homologue with a *tert*-octyl group in the 5 position that imparts higher solubility of both the free and copper-loaded ligand in chloroform. Changing the size of the 5-alkyl substituents in salicylaldoximes has been shown to have only a small effect on the distribution coefficients for copper extraction into hydrocarbon solvents.<sup>23</sup> This also was found to be the case in this work for extractions into chloroform; the pH values for 50% loading ( $pH_{0.5}$ )<sup>23</sup> of 5-*tert*-butyl- and 5-*tert*-octylsalicylaldoximes (1 and 8) are 1.68 and 1.73.

3-Substitution clearly has a major influence on the extractant strength, which is found to follow the order Br > NO<sub>2</sub> > Cl > OMe > Me ≥ H > <sup>t</sup>Bu. The difference in the  $pH_{0.5}$  values for copper loading by the 3-*tert*-butyl- and 3-bromo-substituted extractants, 3 and 6, respectively, represents a difference in the distribution coefficients for copper extraction of two orders of magnitude. Because the potential practical benefits of being able to tune extractant strengths in this way are considerable, it is important to understand the origin of these variations. The introduction of electronegative groups with hydrogen-bond acceptor properties will buttress interligand hydrogen bonding and stabilize the outer coordination sphere. Such substituents will also increase the acidity of the phenol groups, favoring the copper-loading equilibrium.<sup>14</sup> In contrast, they might also be expected to reduce the electron-donor properties of the phenolate oxygen and oximic nitrogen atoms, destabilizing the inner-sphere complex. In the sections below, a combination of structural and computational studies is used to define the relative importance of the effects on the inner and outer coordination spheres of the complexes.

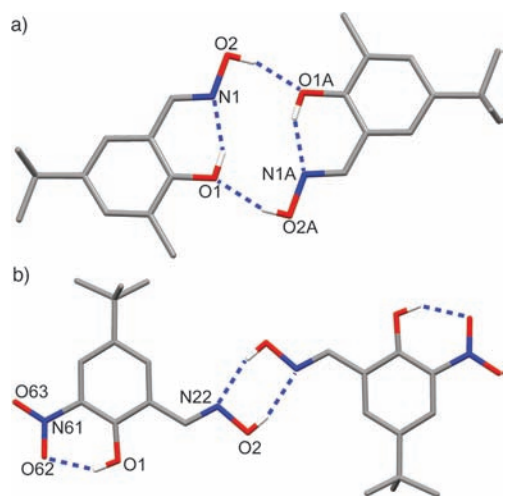
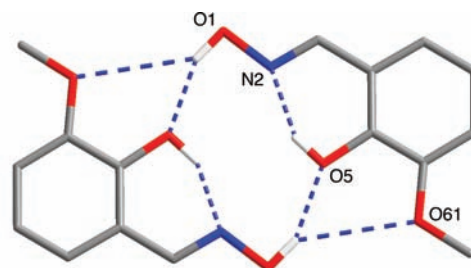


**Figure 4.** (a) Crystal structure of the 14-membered pseudomacrocylic hydrogen-bonded dimer  $[2]_2$ , which has a cavity size = 2.003(2) Å. Analogous hydrogen-bonded dimers are seen in the crystal structures of  $[3]_2$ ,  $[5]_2$ , and  $[6]_2$ , with cavity sizes reported in Figure 5. (b) Crystal structure of the six-membered hydrogen-bonded dimer  $[4]_2$  [ $O2 \cdots N22A = 2.817(1)$  Å]. Hydrogen atoms not involved in hydrogen bonding and solvent molecules have been removed for clarity.

**Dependence of the Solid-State Structures of the Free Ligands on the 3-X Substituent.** In the solid state, most salicylaldoximes form a strong intermolecular hydrogen bond between the oxime hydroxyl group and the phenolic oxygen atom in a neighboring molecule. A head-to-tail arrangement gives dimers with a 14-membered pseudomacrocylic motif (see Figures 2 and 4a), and in some cases, one-dimensional hydrogen-bonded ribbons are formed.<sup>9</sup> Examining the solid-state structures of these dimers allows us to probe the effect of the 3-substituent on the cavity size of the dimer without the added complexities introduced by coordination of a metal ion: the effect of substitution on the intradimer hydrogen-bonding motif, which is similar to that seen in the copper(II) complexes, should dominate. In this work, 10 new crystal structures (see the Supporting Information, S4) of salicylaldoximes (1–9 and 14) were determined, complementing a previous study<sup>22</sup> in which the structures of 10–13 and 15 were analyzed. Compounds 1, 7, and 8 formed the previously described hydrogen-bonded ribbon structure and so will not be discussed in detail (see the Supporting Information, S5).

The very strong hydrogen-bond acceptor properties of the 3-NO<sub>2</sub> group lead to 4 and 9 forming an arrangement not seen previously in salicylaldoxime crystal structures, in which the NO<sub>2</sub> unit acts as a hydrogen-bond acceptor for the phenolic proton. The oxime group retains the *E* configuration seen in the dimer and ribbon structures but is rotated by 180° about the phenylmethine C–C bond to allow the NOH unit to form a hydrogen-bonded six-membered ring with an adjacent oxime moiety (Figure 4b). This six-membered hydrogen-bonded oxime dimer structure has recently been observed in the high-pressure polymorph salicylaldoxime-II. Application of pressure to a single crystal of salicylaldoxime-I, a 14-membered pseudomacrocylic dimer described in detail later, results in a phase change at 5.93 GPa to this new type of structure.<sup>25</sup>

The effects of 3-substitution on hydrogen-bond buttressing were investigated by determining the “cavity sizes”, the average distance of the oxygen and nitrogen donor atoms from their centroid, in the pseudomacrocylic dimers (Figure 5) formed by



Substituent	Ligand	Hole Size / Å <sup>[a]</sup>	pH <sub>-0.5</sub>	Ligand	Hole Size / Å <sup>[a]</sup>
H	1	– <sup>[b]</sup>	1.68	10	2.0048(15)
Me	2	2.003(2)	1.67	11	2.0237(18)
<i>t</i> -Bu	3	2.025(1)	2.64	12	2.0367(19)
Cl	5	1.973(8)	0.91	13	1.9837(12)
Br	6	1.968(8)	0.42	14	1.9726(53)
OMe	7	– <sup>[b]</sup>	1.09	15	1.9492(19)

**Figure 5.** Solid-state structure of  $[15]_2$  showing the interaction  $[H1 \cdots O61 = 2.96(3)$  Å] between the 3-OMe group (O61) and the oximic OH group (O1) and a comparison of the size of the cavity defined by the N<sub>2</sub>O<sub>2</sub> donor set [ $1.9492(19)$  Å] with those in related pseudomacrocylic dimers.<sup>[a]</sup>The mean distance of the oximic nitrogen and phenolic oxygen atoms from their centroid.<sup>[b]</sup>These compounds form assemblies of linear ribbons rather than pseudomacrocylic dimers via intermolecular oximic hydroxyl to phenol oxygen hydrogen bonding (see the Supporting Information).

the 5-*tert*-butyl-substituted ligands, 2, 3, 5, and 6, and their unsubstituted analogues, 10–15. Of the ligands with 5-*t*Bu substituents, the cavity sizes of the solid-state dimers are smaller for 5 (Cl) and 6 (Br), which have groups that can act as hydrogen-bond acceptors and may form bifurcated hydrogen bonds, and larger for 3, which has a bulky *tert*-butyl group, while the intermediate cavity size in 2 (Me) is compatible with the methyl substituent being smaller but unable to accept hydrogen bonds. This provides tentative evidence of the effect that the 3-substituent has on interligand hydrogen bonding, suggesting that the substituent can “buttress” the hydrogen bonds and so possibly stabilize salicylaldoxime dimers.

A more extensive series of dimeric, preorganized ligands is available in the form of the salicylaldoximes 10–15, which carry no substituents in the 5 position. The X-ray crystal structures of 10 and 15 have been reported previously<sup>26,27</sup> but were redetermined and refined under conditions identical with the rest of the series to ensure comparability of the data. In the course of this study, a novel polymorph of 10 was also crystallized that does not show dimer formation (the one-dimensional hydrogen-bonded ribbon structure emerged and so will not be discussed further).<sup>28</sup> 3-Nitrosalicylaldoxime was also prepared, but its insolubility rendered it difficult to purify or crystallize, and the novel hydrogen-bonding arrangement associated with the 3-NO<sub>2</sub> group, which is seen in 4 and 9 (above), suggests that it is unlikely to form dimers of the type shown in Figure 4a. As with the 5-*tert*-butyl-substituted ligands, the cavity sizes of the unsubstituted analogues are smaller when the 3-substituents have hydrogen-bond acceptor properties, and the dependence of the cavity size on the nature of the 3-substituent observed in 2, 3, 5, and 6, Br < Cl < Me < *t*Bu, is reproduced in the more extended series 10–15, OMe < Br < Cl < H < Me < *t*Bu. This order is very similar to the relative extractive efficacies of the ligands 1–9, with the exception of the 3-OMe-substituted compounds.

Interaction energies within the dimers in the solid state (Table 1) were analyzed by the PIXEL method, which models

**Table 1.** Interaction Energies between the Halves of Each of the 3-Substituted Dimers, [11]<sub>2</sub> etc., Relative to Their Unsubstituted Analogue, [10]<sub>2</sub>, Calculated by the PIXEL Method,<sup>29,30</sup> Compared with the DFT-Calculated Gas-Phase Dimerization Enthalpies and Cavity Sizes, Using the Method<sup>33,34</sup> TPSS/6-31++G(d,p) and Corrected for BSSE,<sup>35,36</sup> and also the Measured Cavity Sizes in the Solid State from X-ray Structure Determination and Solvent Extraction Strengths of the Analogous 5-*t*-Bu-Substituted Ligands

	15 (OMe)	14 (Br)	13 (Cl)	10 (H)	11 (Me)	12 ( <i>t</i> Bu)
$E_{\text{Coulombic}}/\text{kJ mol}^{-1}$	-4.8	-2.2	-0.5	0.0	+0.2	+2.1
$E_{\text{repulsion}}/\text{kJ mol}^{-1}$	-0.4	+0.7	0.0	0.0	+0.6	+6.2
$E_{\text{polarization}}/\text{kJ mol}^{-1}$	-1.0	-1.4	-1.0	0.0	-0.8	-2.7
$E_{\text{dispersion}}/\text{kJ mol}^{-1}$	-0.8	-1.3	-1.5	0.0	-1.5	-5.8
$E_{\text{TOTAL}}/\text{kJ mol}^{-1}$	-7.0	-4.2	-3.0	0.0	-1.5	-0.2
cavity radius (XRD)/Å	1.949(2)	1.973(5)	1.982(1)	2.005(1)	2.024(2)	2.037(2)
cavity radius (DFT)/Å	1.972	1.966	1.988	2.005	2.007	2.045
$\Delta H_{\text{dimerization}}/\text{kJ mol}^{-1a}$	-50.2	-45.2	-45.7	-40.7	-39.3	-29.1
pH <sub>0.5</sub> for copper(II) extraction	1.09	0.49	0.91	1.68	1.67	2.64
by related 5- <i>t</i> -Bu ligands	7 (OMe)	6 (Br)	5 (Cl)	1 (H)	2 (Me)	3 ( <i>t</i> Bu)

<sup>a</sup> Theoretical gas-phase dimerization enthalpies are calculated as the difference in energies between the energy-minimized structures of the dimers and the parent monomers, corrected for basis set superposition errors by the counterpoise method.<sup>35,36</sup>

Coulombic-polarization and dispersive-repulsion contributions.<sup>29,30</sup> In order to evaluate the effects of 3-substitution in more detail, differences between the energy contributions,  $E_{\text{Coulombic}}$ , etc., for each crystal structure of 10–15 are presented in Table 1. These “normalized” values demonstrate that the ligands with hydrogen-bond acceptor substituents, 13, 14, and 15, show the most favorable ligand–ligand attraction energies ( $E_{\text{TOTAL}}$  in Table 1). The Coulombic term is favorable in these three dimers, which is consistent with the formation of additional hydrogen-bonding interactions by the X groups. The  $E_{\text{Coulombic}}$  term is most favorable for [15]<sub>2</sub>, which is in accordance with the good hydrogen-bond acceptor properties of the OMe group,<sup>31</sup> despite the much longer (3.72 Å) than ideal distance between the methoxy and phenolic oxygen atoms for a strong hydrogen bond. The term is greater for the bromo-substituted ligand than the chloro-substituted ligand; the larger bromine atom either provides a better hydrogen-bond acceptor than the chlorine atom or is closer to the oxime proton and so a stronger interaction is possible. The large repulsion term ( $E_{\text{repulsion}}$ ) for 12 is consistent with the bulk of the 3-*tert*-butyl substituent and with this ligand dimer having the largest cavity.

In the PIXEL method, the dispersion energy terms are the most difficult to calculate<sup>32</sup> and the favorable values for [11]<sub>2</sub> and [12]<sub>2</sub>, particularly for [12]<sub>2</sub>, may be an artifact, leading to  $E_{\text{TOTAL}}$  values being slightly more favorable than those for the unsubstituted ligand [10]<sub>2</sub>. Density functional theory (DFT)-calculated<sup>33–36</sup> gas-phase dimerization enthalpies are also included in Table 1, and these values also correlate well with the cavity radii observed in the solid state; molecules with hydrogen-bond acceptor substituents in the 3 position have the smallest cavities and the most favorable dimerization enthalpies. With the exception of the methoxy-substituted ligand, 7, the dependence of the dimerization enthalpies on the nature of the 3-X substituents follows the order of the strength of the 5-*tert*-butyl-substituted compounds, 1–9, as copper extractants (pH<sub>0.5</sub> values from Figure 3 are included in Table 1). While the method gives approximately equal values for the dimerization enthalpies of the chloro- and bromo-substituted dimers, [13]<sub>2</sub> and [14]<sub>2</sub>, respectively, the calculated cavity size for [14]<sub>2</sub> is smaller, matching the relationship seen in the order of extractive efficacy. The results suggest that hydrogen-bond buttressing by substituents in the 3 position has a major effect on the ligand

dimerization, which, in turn, enhances their strength as copper(II) extractants. The anomalously weaker extraction by 7 probably relates to the electron-releasing properties of its 3-OMe group, which influences the acidity of the ligand and the strength of the inner-sphere bonds (see below). The fact that 7 is a stronger extractant than the unsubstituted ligand 1 suggests that the 3-OMe group is an effective hydrogen-bond acceptor and buttresses the dimeric assembly.

**Dependence of the Solid-State Structures of Copper(II) Complexes on the 3-X Substituent.** In order to probe the effects of 3-X substituents on the structure and bonding in copper(II) complexes of the salicylaldoxime ligand series, we looked first to their solid-state structures. Single-crystal X-ray structure determinations (see the Supporting Information, S4) of [Cu(1-H)<sub>2</sub>], [Cu(2-H)<sub>2</sub>], [Cu(3-H)<sub>2</sub>], [Cu(4-H)<sub>2</sub>(py)<sub>2</sub>], [Cu(6-H)<sub>2</sub>], and [Cu(7-H)<sub>2</sub>] (py = pyridine) have shown that all contain the pseudomacrocyclic unit with interligand hydrogen bonds typical of bis(salicylaldoximate)copper(II) complexes,<sup>9</sup> but several different supramolecular architectures arise in the solid state from different types of axial contacts to the copper atoms and from packing effects. Such architectures commonly feature face-to-face or edge-to-face association of the [Cu(L-H)<sub>2</sub>] units, with phenoxide or oxime oxygen atoms lying in the axial sites of the planar CuO<sub>2</sub>N<sub>2</sub> units. The association in the solid state through these axial sites perturbs the bond lengths in the inner coordination sphere of the copper atoms via Jahn–Teller effects and, consequently, we would not expect and do not find a correlation between the hole size in the solid state and the relative stabilities of the complexes in solution, as judged by distribution coefficients in solvent extraction and the enthalpies of formation calculated in the gas phase (see below and Table 2).

In [Cu(1-H)<sub>2</sub>], axial contacts between copper(II) atoms and oxime oxygen atoms of adjacent molecules (Figure 6a) define the solid-state structure, which comprises three crystallographically independent half-molecules, each containing a copper(II) atom located on an inversion center. Each copper atom has two oxime oxygen atoms from adjacent molecules in axial positions, giving it an overall Jahn–Teller distorted octahedral coordination sphere and connecting the complex units to form two-dimensional sheets along the *ab* plane. The hexagonal networks of copper, nitrogen, and oxygen atoms are displayed in Figure 6b by

**Table 2. Bond and Contact Distances in the Inner and Outer Spheres of the Solid-State Structures of [Cu(L-H)<sub>2</sub>] Complexes of 1–7**

contact or bond distance (Å)	1 <sup>a</sup> (H)	2 <sup>b</sup> (Me)	3 <sup>b</sup> ( <sup>t</sup> Bu)	4 <sup>b,c</sup> (NO <sub>2</sub> )	6 (OMe)	7 <sup>b</sup> (Br)
Cu–N/Å	1.943(3)	1.936(4)	1.923(8)	1.957(7)	1.954(3)	1.947(4)
Cu–O/Å	1.904(3)	1.881(3)	1.920(8)	1.919(6)	1.885(2)	1.871(4)
hole size/Å	1.924(4)	1.909(5)	1.922(11)	1.938(9)	1.920(4)	1.909(6)
NO...O/Ph/Å	2.583(5)	2.616(6)	2.625(10)	2.655(9)	2.627(4)	2.609(6)
Cu–axial/Å	2.579(4)	3.343(11)	n/a	2.522(6)	n/a	n/a
NO...X/Å	n/a	n/a	n/a	2.933(9)	3.722(2)	3.666(6)
NOH...X/Å	n/a	n/a	n/a	2.305(6)	3.00(4) <sup>d</sup>	2.88(4) <sup>d</sup>

<sup>a</sup> Values are the average of three crystallographically independent half-molecules. <sup>b</sup> Values are the average of two crystallographically independent half-molecules. <sup>c</sup> Bispyridine adduct. <sup>d</sup> From calculated hydrogen-atom positions.

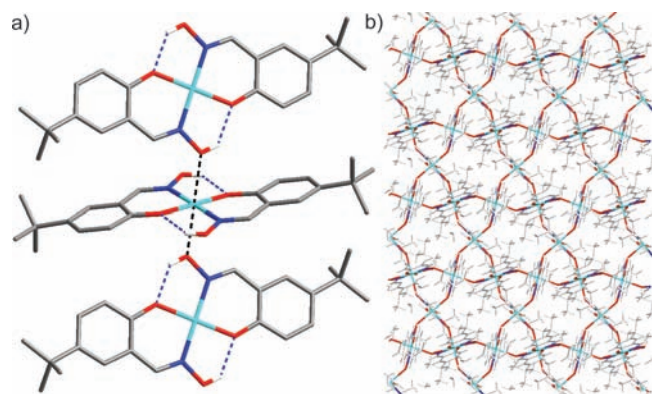


**Figure 6.** Solid-state structure of [Cu(1-H)<sub>2</sub>]. (a) Axial copper(II) contacts in the solid-state structure of [Cu(1-H)<sub>2</sub>] linking the individual complex units (hydrogen atoms not involved in hydrogen bonding have been omitted for clarity). (b) Infinite two-dimensional hexagonal network of copper, nitrogen, and oxygen atoms in the solid-state structure of [Cu(1-H)<sub>2</sub>] viewed down the *c* axis (carbon and hydrogen atoms have been lightened for clarity).

lightening all carbon and hydrogen atoms in the structure and viewing down the *c* axis.

[Cu(2-H)<sub>2</sub>] has two independent molecules in the unit cell, which are positioned directly above each other at a rotation of 45°. A 4<sub>2</sub> axis runs through the copper atoms, parallel to the *c* axis, generating an infinite helical structure, while an inversion center generates a symmetry-related, opposite-handed helix. Distances of 3.345(8) and 3.341(8) Å separate the copper atoms within the helices (Figure 7).

[Cu(3-H)<sub>2</sub>] has no axial interactions. A space-filling diagram of one of the two very similar but crystallographically independent molecules (Figure 8a) shows the 3-*tert*-butyl group and the oximic proton adopting a staggered conformation in order to minimize disruption of the hydrogen bonding without significantly distorting the coordination sphere of the copper center. In the solution phase, it is expected that free rotation of the <sup>t</sup>Bu group would disrupt the stabilizing hydrogen-bonding motif, and this may be the reason that 3 is the weakest extractant. The complex of the 3-NO<sub>2</sub>-substituted ligand, 4, could only be crystallized as the bispyridine adduct, [Cu(4-H)<sub>2</sub>(py)<sub>2</sub>]. Figure 8b illustrates the formation of bifurcated hydrogen bonds in the outer coordination sphere, which are expected to stabilize the molecule<sup>16</sup> and may explain the high extraction strength of its 5-*tert*-octyl-substituted analogue 9. The crystal structures of [Cu(6-H)<sub>2</sub>] and

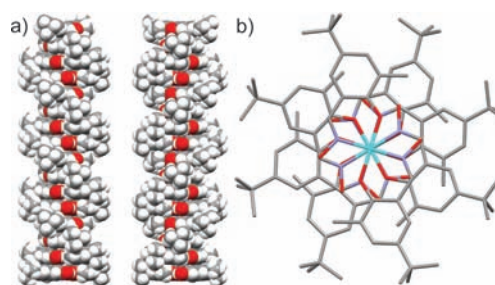


**Figure 7.** (a) Space-filling representation of the left- and right-handed, symmetry-equivalent supramolecular helices of [Cu(2-H)<sub>2</sub>]. (b) View down the *c* axis of one of the helical repeat structures (hydrogen atoms are removed for clarity).

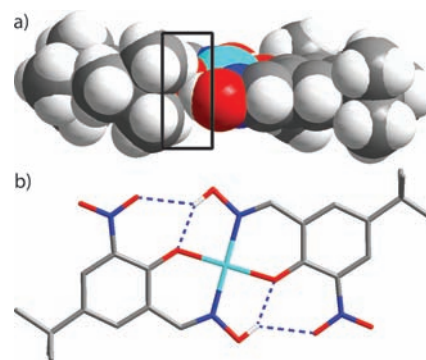


**Figure 8.** (a) Space-filling diagram of one of the crystallographically independent molecules of [Cu(3-H)<sub>2</sub>] observed in its solid-state structure, showing interaction of the 3-<sup>t</sup>Bu substituent with the intra-complex hydrogen-bonding motif. (b) Bifurcated hydrogen bonds in the crystal structure of [Cu(4-H)<sub>2</sub>(py)<sub>2</sub>]. Hydrogen atoms not involved in hydrogen bonding and axially coordinated pyridine molecules have been removed for clarity.

[Cu(7-H)<sub>2</sub>] show no axial contacts with the copper(II) centers but have similar interaction between the hydrogen-bond-accepting Br and OMe substituents and the pseudomacrocyclic hydrogen-bond motif (see the Supporting Information, S6) as seen in [Cu(4-H)<sub>2</sub>(py)<sub>2</sub>].

No simple dependence of the bond and contact distances and cavity sizes in the coordination spheres of the complexes on the nature of the 3-substituents is evident from the data collated in Table 2. The complexes with the two most significant axial interactions, [Cu(1-H)<sub>2</sub>] and [Cu(4-H)<sub>2</sub>(py)<sub>2</sub>], have the largest

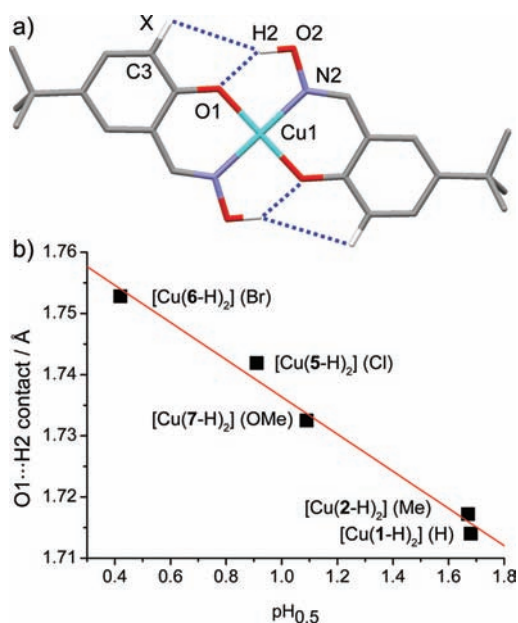


**Figure 9.** (a) Energy-minimized structure (B3LYP/6-31G) of  $[\text{Cu}(\text{1-H})_2]$  with labeling of the relevant atoms of the structure. The same labeling scheme is used in all modeled structures. (b) Correlation between the calculated  $\text{O1}\cdots\text{H2}$  contact distance in the copper(II) complexes and the measured extraction strength of the corresponding free ligands.

cavity sizes, consistent with Jahn–Teller effects. While the *solid-state* structure determinations confirm the formation of pseudo-macrocyclic complexes with strong interligand hydrogen bonding, the differences in axial interactions in the inner coordination spheres of the copper atoms associated with different solid-state packing motifs make it impossible to analyze how variation of the 3-X substituents influences bonding in the inner and outer coordination spheres. Solutions of the complexes gave well-resolved electron paramagnetic resonance (EPR) spectra (see the Supporting Information, S7), but variations in the hyperfine coupling showed only a very small dependence on the nature of the 3-X substituents and ENDOR measurements are currently being undertaken to probe proton environments in the outer coordination spheres. Much more useful information was obtained by calculating and comparing structures in the gas phase using DFT methods (see below).

**Dependence of the Calculated Structures of the Copper Complexes and the Strength of the Extractants on the Nature of the 3-X Substituent.** Calculations (see the Supporting Information, S8) were undertaken on isolated  $[\text{Cu}(\text{L-H})_2]$  complexes of ligands 1–7, initially using the DFT method<sup>37–40</sup> B3LYP/6-31G. Frequency calculations were carried out on all optimized structures to ensure that an energy minimum had been attained. As expected, variations in the cavity sizes across the series of complexes having ligands with different 3-substituents (see the Supporting Information, Table S2) are smaller in comparison with those for the free ligand dimers, but there are some significant variations in the *relative* lengths of the Cu–O and Cu–N bonds. In contrast to the other complexes, in the energy-minimized structure of  $[\text{Cu}(\text{3-H})_2]$ , which contains the bulky 3-*tert*-butyl substituent, the Cu–O bond (1.928 Å) is longer than the Cu–N bond (1.914 Å). This can be attributed to steric hindrance *ortho* to the phenoxide group.

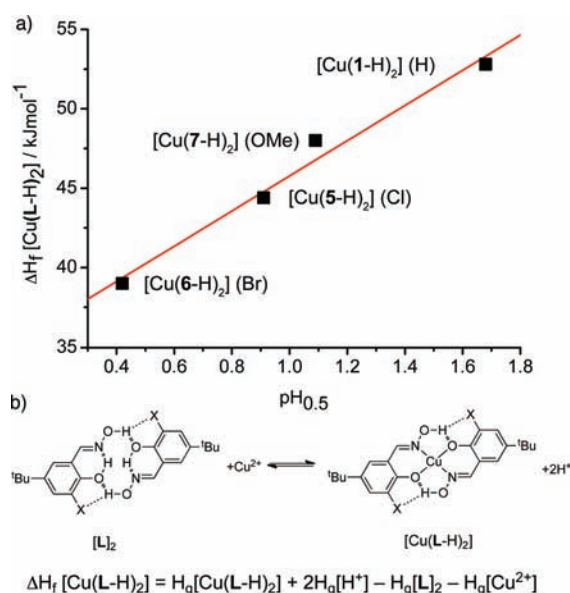


**Figure 10.** a) The correlation between calculated (B3LYP/6-31+G(d,p)) enthalpies of formation ( $\Delta H_f$ ) of the copper(II) complexes in the gas phase with the measured extraction strength ( $\text{pH}_{0.5}$ ) of the corresponding free ligands. b) The equilibrium and equation used to calculate the  $\Delta H_f$  values.

Outer-sphere interactions, and in particular hydrogen-bond buttressing, appear to influence the calculated structures. For ligands with a similarly sized<sup>41</sup> 3-substituent, namely, 1 (H), 2 (Me), 5 (Cl), 6 (Br), and 7 (OMe), the formation of an additional weak hydrogen bond to the 3-X atoms via the five-membered ring motif shown in Figure 9a pulls the oximic hydrogen atom (H2) away from the phenolate oxygen atom (O1), lengthening the  $\text{O1}\cdots\text{H2}$  contact distance. The efficacy of the 3-substituent in forming bifurcated hydrogen bonds in this way is dependent on its size: a correlation is observed (see the Supporting Information, S8) between the increased extractant strength of the ligand and the van der Waals radii<sup>42</sup> of the 3-substituent.<sup>43</sup> This size dependence is also observed in the energy-minimized structures of the salicylaldoxime dimers (Table 1) and may explain the increased extractive efficacy of the 3-bromo-substituted ligand, 6, in comparison to its 3-chloro-substituted counterpart, 5. While it may seem counterintuitive that lengthening intracomplex hydrogen bonds results in stabilization of the copper(II) complex, it is the overall stabilizing effect of forming *bifurcated* hydrogen bonds rather than single hydrogen bonds that must be considered, and there exists a strong correlation between the *measured* extractant strength and the *calculated*  $\text{O1}\cdots\text{H2}$  intracomplex hydrogen-bond distance.

In order to probe whether this remarkable correlation is indeed due to variation of the buttressing properties of the 3-X substituents rather than their inductive effects on the bonding in the inner sphere of the complexes or their influence on the acidity of the phenolic ligands, higher level DFT calculations were performed using the DFT method B3LYP/6-31+G(d,p) on the complexes  $[\text{Cu}(\text{5-H})_2]$ ,  $[\text{Cu}(\text{6-H})_2]$ , and  $[\text{Cu}(\text{7-H})_2]$  in comparison with the control complex  $[\text{Cu}(\text{1-H})_2]$ . The enthalpies of formation of these complexes,  $\Delta H_f$ , were calculated from the enthalpy-corrected energies of the optimized structures,  $H_g$ , for the species in Figure 10 (for all data, see the Supporting Information, Table S3).

The endothermic nature of the *gas-phase* formation reactions required to form the copper(II) complexes is to be expected because the process requires the release of two protons. In *solution*, the high free energy of hydration of these protons is a major factor in making extraction of  $\text{Cu}^{2+}$  from, and release of protons to, the aqueous phase thermodynamically favorable. Nevertheless, the relative order of ease of formation of the copper complexes in the gas phase as judged by the calculated  $\Delta H_f$  values ( $[\text{Cu}(6\text{-H})_2] > [\text{Cu}(5\text{-H})_2] > [\text{Cu}(7\text{-H})_2] > [\text{Cu}(1\text{-H})_2]$ ) is the same as the order of strength of the ligands as copper(II) extractants as judged by the measured  $\text{pH}_{0.5}$  values (Figure 10). The importance of 3-substitution on outer-sphere interactions in bis(salicylaldoximate) complexes in the gas phase has also been observed for monoanions formed by deprotonation of one of the oxime groups in the gas phase during collision-induced dissociation mass spectrometric experiments.<sup>44</sup> A breakdown of the steps associated with gas-phase formation of the complexes (see the Supporting Information, S8) indicates that while deprotonation of the methoxy-substituted ligand 7 is less favorable, as might be expected from the electron-releasing properties of the 3-OMe group, both hydrogen-bond buttressing (see also Table 1) and formation of the inner-sphere complexes are more favorable.

## CONCLUSIONS

The preparation of a series of ligands with substituents that can provide both favorable and unfavorable effects on interligand hydrogen bonding has allowed us to demonstrate the importance of outer-sphere coordination chemistry in the performance of reagents that are used on kilotonne scales in the hydrometallurgical production of base metals. The results have identified an effective strategy for extractant design in which the strength and selectivity of metal recovery is controlled by exploiting interligand hydrogen bonding. For the ligands in this work, the distribution coefficient for copper(II) extraction has been varied by more than 2 orders of magnitude. Ligand–ligand interactions present in the outer coordination sphere are observed in the solid-state structures of ligand dimers and could also be evaluated through DFT calculations. The importance of such supramolecular effects in commercial solvent extraction processes results from the use of low-polarity water-immiscible solvents, such as kerosenes, which do not compete with inner- or outer-sphere hydrogen-bond donors and acceptors. The low solvation energies of species in the organic phase, and/or the similarities of solvation enthalpies of the preorganized ligand dimers and their copper(II) complexes, also lead to a remarkable correlation between the order of the calculated enthalpies of formation of the preorganized ligand dimers and of their copper complexes in the gas phase and the observed strength of the ligands as copper solvent extractants. We are currently exploiting this phenomenon in other ligand systems.

## ASSOCIATED CONTENT

**S** Supporting Information. Synthesis of ligands, precursors, and copper(II) complexes, experimental details of solvent extraction and EPR spectroscopy, all crystallographic data, and DFT analysis of copper(II) complexes. This material is available free of charge via the Internet at <http://pubs.acs.org>.

## AUTHOR INFORMATION

### Corresponding Author

\*E-mail: [p.a.tasker@ed.ac.uk](mailto:p.a.tasker@ed.ac.uk)

## ACKNOWLEDGMENT

The authors thank EPSRC, CCDC, and University of Edinburgh for funding and Dr. Andrew Turner at the EastCHEM Research Computing Facility for assistance with DFT calculations.

## REFERENCES

- (1) Tasker, P. A.; Plieger, P. G.; West, L. C. *Compr. Coord. Chem. II* **2004**, *9*, 759–808.
- (2) Nicol, M. J.; Fleming, C. A.; Preston, J. S. *Compr. Coord. Chem.* **1987**, *6*, 779–942.
- (3) Irving, H. M.; Williams, R. J. P. *J. Chem. Soc.* **1953**, 3192–3210.
- (4) Cole, P. M.; Sole, K. C.; Feather, A. M. *Tsinghua Sci. Technol.* **2006**, *11*, 153–159.
- (5) Sole, K. C.; Feather, A. M.; Cole, P. M. *Hydrometallurgy* **2005**, *78*, 52–78.
- (6) Outer-sphere interactions are also known to stabilize metal complexes outwith the field of hydrometallurgy. For example, a considerable increase in the stability is afforded to bis(2,9-diphenyl-1,10-phenanthroline)copper(I) complexes, through interligand  $\pi$  stacking, when compared to their unsubstituted analogues. See: Cesario, M.; Dietrich-Buchecker, C. O.; Guilhem, P.; Pascard, C.; Sauvage, J.-P. *Chem. Commun.* **1985**, 244–247.
- (7) Mackey, P. J. *CIM Magazine* **2007**, *2*, 35–42.
- (8) Kordosky, G. A. *Proceedings of the International Solvent Extraction Conference*, Cape Town, South Africa, March 17–21, 2002; ISEC: 2002; pp 853–862.
- (9) Smith, A. G.; Tasker, P. A.; White, D. J. *Coord. Chem. Rev.* **2003**, *241*, 61–85.
- (10) pH adjustment in conventional mixer settlers or between stages of extraction is not favored because it is often difficult to control and the addition of base generates salts that have to be removed from the system and adversely affect the material balance of the flowsheet.
- (11) Szymanowski, J. *Hydroxyoximes and Copper Hydrometallurgy*; CRC Press: Boca Raton, FL, 1993.
- (12) Parrish, J. R. *J. S. Afr. Chem. Inst.* **1970**, *23*, 129–135.
- (13) Lakshmanan, V. I.; Lawson, G. J. *J. Inorg. Nucl. Chem.* **1975**, *37*, 207–209.
- (14) Szymanowski, J.; Borowiak-Resterna, A. *Crit. Rev. Anal. Chem.* **1991**, *22*, 519–566.
- (15) Burger, K.; Egyed, I. *Magy. Kem. Foly.* **1965**, *71*, 143–149.
- (16) Burger, K.; Ruff, F.; Ruff, I.; Egyed, I. *Magy. Kem. Foly.* **1965**, *71*, 282–291.
- (17) Forgan, R. S.; Wood, P. A.; Campbell, J.; Henderson, D. K.; McAllister, F. E.; Parsons, S.; Pidcock, E.; Swart, R. M.; Tasker, P. A. *Chem. Commun.* **2007**, 4940–4942.
- (18) Aldred, R.; Johnston, R.; Levin, D.; Neilan, J. *J. Chem. Soc., Perkin Trans. 1* **1994**, 1823–1831.
- (19) Masilamani, D.; Rogic, M. M. *J. Org. Chem.* **1981**, *46*, 4486–4489.
- (20) Michel, F.; Thomas, F.; Hamman, S.; Saint-Aman, E.; Bucher, C.; Pierre, J.-L. *Chem.—Eur. J.* **2004**, *10*, 4115–4125.
- (21) Lindoy, L. F.; Meehan, G. V.; Svenstrup, N. *Synthesis* **1998**, 1029–1032.
- (22) Wood, P. A.; Forgan, R. S.; Lennie, A. R.; Parsons, S.; Pidcock, E.; Tasker, P. A.; Warren, J. E. *CrystEngComm* **2008**, *10*, 239–251.
- (23) Stepniak-Biniakiewicz, D.; Szymanowski, J. *Hydrometallurgy* **1981**, *7*, 299–313.
- (24) The  $\text{pH}_{0.5}$  value is the pH of the aqueous phase at which the ligand in the organic phase reaches 50% capacity for the species being extracted, in this case copper, and is used as a standard term to compare the strength of the extraction of a series of ligands.<sup>11</sup> In order for  $\text{pH}_{0.5}$

values to be comparable, identical experimental conditions must be used for extractions for the complete ligand series.

(25) Wood, P. A.; Forgan, R. S.; Henderson, D.; Parsons, S.; Pidcock, E.; Tasker, P. A.; Warren, J. E. *Acta Crystallogr., Sect. B* **2006**, *62*, 1099–1111.

(26) Pfluger, C. E.; Harlow, R. L. *Acta Crystallogr., Sect. B* **1973**, *29*, 2608–2609.

(27) Xu, T.; Li, L.-Z.; Ji, H.-W. *Hecheng Huaxue* **2004**, *12*, 22–24.

(28) Wood, P. A.; Forgan, R. S.; Parsons, S.; Pidcock, E.; Tasker, P. A. *Acta Crystallogr., Sect. E* **2006**, *62*, o3944–o3946.

(29) Dunitz, J. D.; Gavezzotti, A. *Angew. Chem., Int. Ed.* **2005**, *44*, 1766–1787.

(30) Gavezzotti, A. *Struct. Chem.* **2005**, *220*, 499–510.

(31) Palusiak, M.; Grabowski, S. J. *J. Mol. Struct.* **2002**, *642*, 97–104.

(32) Gavezzotti, A. Personal communication, 2007.

(33) Tao, J.; Perdew, J. P.; Staroverov, V. N.; Scuseria, G. E. *Phys. Rev. Lett.* **2003**, *91*, 146401.

(34) Staroverov, V. N.; Scuseria, G. E.; Tao, J.; Perdew, J. P. *J. Chem. Phys.* **2003**, *119*, 12129–12137.

(35) Boys, S. F.; Bernardi, F. *Mol. Phys.* **1970**, *19*, 553–566.

(36) Simon, S.; Duran, M.; Dannenberg, J. J. *J. Chem. Phys.* **1996**, *105*, 11024–11031.

(37) Becke, A. D. *J. Chem. Phys.* **1993**, *98*, 5648–5652.

(38) Lee, C.; Yang, W.; Parr, R. G. *Phys. Rev. B* **1988**, *37*, 785–789.

(39) Stephens, P. J.; Devlin, F. J.; Chabalowski, C. F.; Frisch, M. J. *J. Phys. Chem.* **1994**, *98*, 11623–11627.

(40) Vosko, S. H.; Wilk, L.; Nusair, M. *Can. J. Phys.* **1980**, *58*, 1200–1211.

(41) This correlation cannot be extended to the 3-<sup>t</sup>Bu-substituted ligand, **3**, or the 3-NO<sub>2</sub>-substituted ligand, **4**. In [Cu(3-H)<sub>2</sub>], the O1···H2 contact distance is substantially lengthened as a result of the steric hindrance of the 3-<sup>t</sup>Bu group, while in [Cu(4-H)<sub>2</sub>], the 3-NO<sub>2</sub> group forms a six-membered rather than a five-membered bifurcated hydrogen-bonded system, and so its effect on the O1···H2 distance is not comparable.

(42) Bondi, A. *J. Phys. Chem.* **1964**, *68*, 441–451.

(43) In the case of ligand **7**, which contains a 3-OMe group, the correlation is made with the van der Waals radius of the oxygen atom only; it is assumed that free rotation around the O–C bond means that no significant interaction of the methyl group with the hydrogen bonding will occur.

(44) Roach, B. D.; Forgan, R. S.; Tasker, P. A.; Swart, R. M.; Campbell, J.; McAllister, F. E.; Stopford, A. P.; Duncombe, B. J. *Dalton Trans.* **2010**, *39*, 5614–5616.